Thermochimica Acta, 112 (1987) 221–229
Elsevier Science Publishers B.V., Amsterdam – Printed in The Netherlands

STUDIES ON THE REDUCTION OF IRON/TUNGSTEN MIXED OXIDES

G.C. MAITI [2], U. LÖCHNER [1] and M. BAERNS [1]

[1] *Ruhr-Universität Bochum, Lehrstuhl für Technische Chemie, POB 102148, D-4630 Bochum (F.R.G.)*
[2] *Physics Research Wing, Projects & Development India Ltd., P.O. Sindri, Pin 828122, Dhanbad, Bihar (India)*

(Received 2 July 1986)

ABSTRACT

Structural changes of coprecipitated and mechanically mixed iron/tungsten oxides during calcination and reduction were studied by DTA and XRD. The oven-dried precipitated mass is poorly crystalline towards X-ray diffraction studies and does not crystallize until heat treatment above 400°C. XRD studies indicate the formation of "$Fe_2W_3O_{12}$" [not $Fe_2(WO_4)_3$] as major phase along with a minor amount of WO_3 at 450°C. Above that temperature "$Fe_2W_3O_{12}$" decomposes into Fe_2WO_6 and WO_3. The reduction of "$Fe_2W_3O_{12}$" proceeds through the formation of $FeWO_4$. On complete reduction it forms a mixed lattice of iron and tungsten. Free tungsten oxide is also simultaneously reduced to elemental tungsten via the formation of intermediate oxides.

INTRODUCTION

One of the major problems in Fischer–Tropsch synthesis is often the rapid deactivation of the iron/iron oxide catalytic mass due to the presence of sulphur compounds in the synthesis gas which are produced by coal gasification [1,2]. Several attempts have been made to develop more stable catalysts containing MoO_3 and WO_3, which possess a higher sulphur tolerance [3,4]. Iron molybdates and iron tungstates are also of importance as catalysts for methanol oxidation [5–9].

Surprisingly, there is only scant information on the reduction of Fe_2O_3–WO_3 mixed oxides [10,11], though reduction of pure WO_3 [12,13] and, of course, Fe_2O_3 is well documented [14–16]. A high-pressure study of the WO_3–Fe system with bronze-like $Fe_{0.1}WO_3$ phases has been described [17]. Colour changes occurring under illumination and during cathodic reduction of iron tungstates [18], as well as electric and magnetic effects in these materials [18–20,29,60], have been used to construct opto-electronic devices [21]. Such properties bear no relevance for possible applications of these substances in catalytic processes.

0040-6031/87/$03.50

In the present study we have investigated the nature of structural changes of Fe_2O_3–WO_3 mixed oxides by DTA and XRD in order to follow the course of their reduction down to the elemental stage, along with a careful survey of the literature available on the Fe–W–O system (only the latest and most relevant publications are cited, further references can be found therein). A similar study on the nature of reduction of the Fe_2O_3–MoO_3 system was made earlier [22].

EXPERIMENTAL

Reactants and sample preparation

Coprecipitation. An ammonium tungstate solution (0.15 M) was prepared by dissolving WO_3 in concentrated ammonia (4 h, reflux) and diluting with water to 7 wt% NH_4OH. Portions of this solution were admixed with $Fe(NO_3)_3 \cdot 9H_2O$ solution (0.15 M, $V = 5$ ml s^{-1}) with both solutions at 70°C. The pH was then adjusted to 1.5 within 60 s (65 wt% nitric acid) whereby precipitation occurred. The precipitated mass was neutralized to pH 6 with concentrated ammonia, filtered and washed thoroughly with distilled water. Continuous preparation could not be achieved because of the pH conditions necessary for preparation. The washed mass was oven-dried at 120°C and used for further studies. Chemical analyses gave a composition of 42 at% Fe and 58 at% W for the precipitated mass, designated as sample A.

Mechanical mixture. Such a mixture of equimolar iron oxide and tungsten oxide (reagent grade) was also prepared and is designated as sample B.

Calcination and reduction / DTA

The washed precipitated mass was first calcined in air at 450°C for 1 h. Loss of water and sublimation of white ammonia salt (free from iron or tungsten) up to 400°C resulted in a total weight loss of 32%. To determine the nature of the reduction process the samples were calcined up to 450°C under argon and then exposed to hydrogen for reduction. Differential thermal analysis measurements were performed with a controlled-atmosphere differential thermal analyser (Du Pont DTA 990). The samples and α-Al_2O_3 used as a standard were placed in two different gold cups. During calcination and reduction the temperature was increased by 10°C min^{-1}. A sample of about 15 mg was used in each experiment.

X-ray diffraction

X-ray diffraction patterns were recorded with a Guinier-chamber Huber 621 with an evacuable protective gas cap using monochromatized Fe-$K\alpha_1$

radiation (operating conditions: 50 kV, 20 mA) and single-screen X-ray-film Kodak SB-392. Silicon was used as an internal standard for the correction of the angles derived from the diffraction lines. The crystal phase composition of the samples was determined by comparing the measured *d*-spacings with standard ASTM values [23]. The lattice parameter of iron–tungsten solid solution [41] was determined from corrected values using a suitable computer program. To avoid any interaction between the samples and ambient atmosphere before and during X-ray measurements, the samples were handled under inert gas and coated with collodion after they had been subjected to reduction. It has been confirmed that no oxidation of the samples occurred during handling.

RESULTS AND DISCUSSION

Calcination

The DTA curve obtained during calcination of the precipitated mass (sample A, Fig. 1A) shows two endothermic peaks at 110 and 220°C and two exothermic peaks with maxima at 370 and 460°C.

Dehydration is completed around 300°C, up to which temperature the sample is poorly crystalline. The two endothermic peaks below 300°C can be assigned to the removal of absorbed and coordinated water molecules in two steps. In the first step around 110°C intercalated water molecules are removed from between the layers of corner-linked WO_6 octahedra [24,25], while water molecules or hydroxyl groups coordinated to tungsten as parts

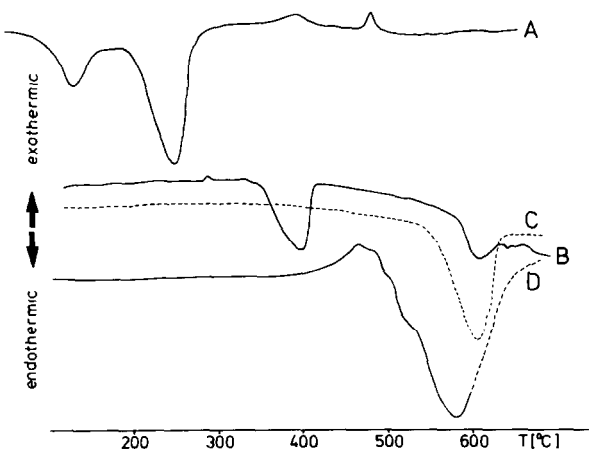

Fig. 1. DSC curves of sample A under calcination (A) and reduction (D), sample B under reduction (B) and pure WO_3 under reduction (C).

TABLE 1

Crystal phase composition of samples A and B

Calcination			Reduction		
Temp. (°C)	Duration (h)	Crystal phase	Temp. (°C)	Duration (h)	Crystal phase
Sample A					
120	10	poorly crystalline	–		
300	5	poorly crystalline	–		
400	5	"$Fe_2W_3O_{12}\cdot xH_2O$"			
		WO_3 (poorly crystalline)	450	12	$FeWO_4$, WO_2
			600	12	WO_2, W
450	5	"$Fe_2W_3O_{12}$"	450	12	$FeWO_4$, WO_2
			600	50	W, WO_2 (minor)
600	5	Fe_2WO_6, WO_3	600	50	W, WO_2 (trace)
Sample B					
600	10	α-Fe_2O_3, WO_3	600	50	W, Fe

of these octahedra remain in the lattice. These are driven off at 220°C, where the hydrated lattice collapses and the composite mass remains non-crystalline (confirmed by XRD patterns) up to 370°C. From there, the ensuing small exothermic peak can be assigned to the crystallization process of "$Fe_2W_3O_{12}$" [26] (not isomorphous with $Fe_2(MoO_4)_3$). For structural reasons and to avoid confusion we prefer this formulation as a ternary oxide to the common formulation as "true" $Fe_2(WO_4)_3$ (isomorphous with $Fe_2(MoO_4)_3$), which has been fully characterized only very recently [6]. At 400°C "$Fe_2W_3O_{12}$" and some poorly crystalline WO_3 [27] can be identified as constituents of the X-ray pattern (Table 1). Further heating results in the decomposition of "$Fe_2W_3O_{12}$" at 450–470°C with no other thermic effect being observed up to 600°C. X-ray investigation of the crystal phase composition at that temperature establishes Fe_2WO_6 [28–31] and WO_3 as the decomposition products. Obviously, small amounts of WO_3 not formed by decomposition but precipitated separately during dehydration of the mixed oxide mass are included within the total amount of WO_3 observed in the residual product at 600°C.

For sample B no solid-state interaction between Fe_2O_3 and WO_3 has been observed on heat treatment of the mechanically mixed oxides up to 600°C, as other authors have also concluded from calorimetric experiments much earlier [32]. Solid-state reaction between these oxides does not start until 760°C [33].

Full reduction

Whereas the reduction of a mechanical mixture of Fe_2O_3 and WO_3 (sample B) proceeds directly into pure elemental iron and tungsten (Fig. 1B,

endothermic peaks at 395 and 605°C, respectively), the reduction behaviour of the iron–tungsten oxides obtained from the coprecipitated mass is much more complicated. For sample B, the measured lattice parameters of the elemental tungsten ($a = 0.3165(3)$ nm) and iron ($a = 0.2866(2)$ nm) formed after reduction at 600°C suggest that no bimetallic lattice or alloy has been formed in this case. This is well in accord with the reported formation of Fe_2W, Fe_7W_6 or an Fe/W-sigma phase only above 900°C [34–39] and with the reported recrystallization of amorphous Fe–W films from room-temperature RF-sputter deposition only above 600°C [40]. The endothermic reaction for the reduction of pure WO_3 to elemental tungsten at 605°C has also been verified from a DTA curve for WO_3 (Fig. 1C). A solid solution of tungsten in α-iron extending to ca. 10 at% tungsten is not to be expected, as it occurs only in high-temperature samples above 1200°C [41].

On the other hand, reduction at 600°C of sample A (pre-calcined at 450°C), resulted in the formation of apparently single-phase elemental tungsten as major reduction product with a minor amount of WO_2 [42]. The crystalline WO_2 also persisted if the sample was pre-calcined at 600°C before starting reduction. The XRD patterns did not indicate the formation of any separate elemental iron phase. Rather, elemental iron remains in a dispersed state within the tungsten lattice, causing an extra broadening of the diffraction lines for elemental tungsten. For iron atoms ion-implanted into tungsten, the occupation of interstitials of the tungsten lattice at random has been confirmed by Mössbauer spectroscopy [43]. A routine Mössbauer spectrum of our sample failed to reveal a free-iron lattice, nor could $FeWO_4$ [44], a spinel or a wustite lattice be identified. We believe, instead, that a true solid solution effect has been achieved on the tungsten-rich side of the Fe–W system by way of treatment of our samples. The measured lattice parameter from the tungsten diffraction lines ($a = 0.3145(3)$ nm) compares to the reported lattice parameter of pure tungsten ($a = 0.31651(3)$ nm) and shows a significant contraction of the tungsten lattice. This could hardly be expected if free interstitials were occupied by the smaller iron atoms (the atomic radii for tungsten and iron calculated from the atomic volumes are 0.1558 and 0.1412 nm, respectively [45]).

Partial reduction

The nature of the mixed oxides leading to a bimetallic tungsten/iron lattice upon reduction remains to be explained. Figure 1D shows the DTA curve for the reduction of sample A starting at 400°C after calcination. An exothermic peak at 465°C with a shoulder at 490°C (weak in nature) is apparent, followed by a strong endothermic peak with maximum at 585°C and with shoulders on the upward slope between 500 and 520°C. Together with the XRD patterns taken at various temperatures and after two different

reduction times (Table 1) and with an evaluation of the available literature on the system the following picture of reduction behaviour emerges.

Reduction of coprecipitated iron–tungsten mixed oxides below 500°C yields $FeWO_4$ [46,47] and WO_2 as crystalline phases. Theoretically, $FeWO_4$ (mineralogically also known as ferberite) can form over a wide temperature range, even at room temperature [32]. Under non-reductive conditions it melts congruently as high as 990°C and undergoes no phase transformations [48].

Both "$Fe_2W_3O_{12}$" and Fe_2WO_6 present at temperatures between 460 and 520°C (one being the decomposition product of the other) upon reduction yield $FeWO_4$, but the reduction of the Fe_2WO_6 phase occurs more readily compared to that of the "$Fe_2W_3O_{12}$" phase (Table 1). It seems that the orthorhombic lattice of Fe_2WO_6 is more easily reducible as compared to that of the tetragonal "$Fe_2W_3O_{12}$" phase.

The reduction of WO_3, formed as a decomposition product of "$Fe_2W_3O_{12}$" as well as directly through dehydration of tungstic acid precursors, yields WO_2 through a series of complicated intermediate oxides with crystallographic shear structures [49–53], depending on the individual reduction conditions.

The presence of poorly crystalline cubic $FeW_2O_7 \cdot nH_2O$ $(0 < n < 2.5)$ oxides (not detectable in our study), which themselves decompose into $FeWO_4$ and WO_3 upon complete dehydration, may add to the complexity of the reduction picture. These oxides can continuously and reversibly take up and lose water between 70 and 500°C [54,55].

Although Fe_2WO_6 coexists with $FeWO_4$ at 1000°C [56] and can be obtained in air up to 1200°C [7,57], above about 520°C $FeWO_4$ is the only stable mixed oxide under reducing conditions. It is slowly reduced into a bimetallic solid solution lattice consisting of tungsten and iron under the employed reaction conditions as described above. This reduction occurs simultaneously with the reduction of WO_3 in the endothermic zone up to 585°C. In this zone, contributions of intermediate "FeO" [58] to the final formation of the mixed metallic lattice cannot be excluded. Contrary to the inertness of Fe_2O_3/WO_3 mixtures, Tamann and others have noted a strong reaction between FeO and WO_3 [32,59,60].

Thus, we ascribe the first exothermic reaction in the DTA curve of Fig. 1D between 400 and 470°C to the reduction of "$Fe_2W_3O_{12}$" into $FeWO_4$, and the broad, structured endothermic peak with maximum at 585°C to a combination of interwoven solid-state decomposition and reduction processes. A careful study with close scrutiny of this zone by thermal, high-temperature X-ray and spectral methods will be needed to clarify all the factors involved.

CONCLUSION

The results of the present study indicate that a bimetallic catalyst consisting of iron and tungsten can be prepared from mixed oxide composites obtained by precipitation techniques at low temperature.

From a catalytic point of view, it appears interesting to study the performance of these catalysts for the hydrogenation of carbon monoxide to Fischer–Tropsch products in the presence of sulphur compounds which are usually considered as catalyst poisons. It may be expected that iron/tungsten catalysts deactivate less by sulphur poisoning than pure iron catalysts. Furthermore, promotion of such catalysts with lithium is likely to modify their synthetic properties without affecting their bulk structure morphology [61].

ACKNOWLEDGEMENTS

This work has been partly supported by the Minister of Research and Technology of the Federal Republic of Germany. We thank Dr. R. Malessa for help with the preparation of the catalysts and Prof. Flörke of the Lehrstuhl für Mineralogie of the Ruhr-Universität for providing XRD facilities.

REFERENCES

1 R.J. Madon and H. Shaw, Catal. Rev. Sci. Eng., 15 (1977) 69.
2 C.H. Bartholomew and J.R. Katzer, Catalyst Deactivation, Elsevier, Amsterdam, 1980, p. 375.
3 J.F. Schultz, F.S. Carn and R.B. Anderson, Noble Metals, Molybdenum and Tungsten in Hydrocarbon Synthesis, AC-Publ., New York, 1972.
4 D.L. Trimm, Design of Industrial Catalysts, Elsevier, Amsterdam, 1980.
5 C.J. Machiels, U. Chowdhry and A.W. Sleight, Prepr. Am. Chem. Soc., Div. Pet. Chem., 28 (1983) 1293.
6 W.T.A. Harrison, U. Chowdhry, C.J. Machiels, A.W. Sleight and A.K. Cheetham, J. Solid State Chem., 60 (1985) 101.
7 U.S. Patent 3165419 (1/12/1965); Chem. Abstr., 62 (1965) P8708a.
8 T. Popov, Proc. 4th Int. Symp. on Heterogeneous Catalysis, Sofia, Bulgaria, 1979, p. 291.
9 A. Swinarski and W. Klafkowski, Rev. Roum. Chim., 23 (1978) 171.
10 I.D. Radomyselskii and L.F. Barchchevskaya, Poroshk. Metall., 10 (1974) 14.
11 V.A. Obrubov, V.P. Shchukin and A.Ya. Averbukh, Zh. Prikl. Khim. (Leningrad), 53 (1980) 507.
12 B. Phillips and L.L.Y. Chang, Trans. AIME, 230 (1964) 1203.
13 A. Magneli, in L. Eyring and M. O'Keeffe (Eds.), The Chemistry of Extended Defects in Non-metallic Solids, North Holland, Amsterdam, 1970, p. 147 ff.
14 P. Barret, in Reactivity of Solids, Proc. 5th Int. Symp. on Reactivity of Solids, Elsevier, Amsterdam, 1964, p. 442.

15 M.S. Whittingham and P.G. Dickens, in Reactivity of Solids, Proc. 7th Int. Symp. on Reactivity of Solids, Chapman and Hall, London, 1972, p. 640.
16 P.A. Vernhovodov, L.D. Konchakovskaya, A.P. Kresanova, R.V. Minakova and I.V. Uvarova, Poroshk. Metall., 4 (1979) 8.
17 I.J. McColm, R. Steadman and S.J. Wilson, J. Solid State Chem., 23 (1978) 33.
18 H. Leiva, K. Dwight and A. Wold, J. Solid State Chem., 42 (1982) 41.
19 R. Bharati and R.A. Singh, J. Mater. Sci., 16 (1981) 511.
20 K. Tennakone and W.G.D. Dharmaratna, J. Chem. Soc., Faraday Trans. 2, 78 (1982) 1699.
21 Japanese Patent 59/81628 (5/11/1984); Chem. Abstr., 102 (1984) 54009c.
22 G.C. Maiti, R. Malessa and M. Baerns, Thermochim. Acta, 80 (1984) 11.
23 ASTM Powder Diffraction File, JCPDS, International Centre for Diffraction Data, Swarthmore, PA, U.S.A.
24 R. Allmann, Acta Crystallogr., Sect. B, 27 (1971) 1393.
25 M.T. Pope and B.W. Dale, Quart. Rev. Chem. Soc., 22 (1968) 527.
26 N. Pernicone and G. Fagherazzi, J. Inorg. Nucl. Chem., 31 (1969) 3323.
27 B.O. Loopstra and P. Boldrini, Acta Crystallogr., Sect. B, 25 (1969) 1420; ref. 36, p. 75 ff.
28 J. Senegas and J. Galy, J. Solid State Chem., 10 (1974) 5.
29 H. Pinto, M. Melamud and H. Shaked, Acta Crystallogr., Sect. A, 33 (1977) 663.
30 C. Parant, J.C. Bernier and A. Michel, C.R. Acad. Sci., Ser. C, 276 (1973) 495.
31 T.S.S. Kumar, R.M. Mallya and M.S. Hegde, Proc. Nucl. Phys. Solid State Phys. Symp., 25C (1982, Publ. 1984) 408.
32 G. Tamann, Z. Anorg. Allg. Chem., 149 (1925) 21.
33 G. Bayer, Ber. Dtsch. Keram. Ges., 39 (1962) 535.
34 J.O. Andersson, CALPHAD: Comput. Coupling Phase Diagrams Termochem., 7 (1983) 317.
35 L. Repiska, L. Komorova and Z. Baffyova, Zb. Ved. Pr. Vys. Sk. Tech. Kosiciach, (1982, Publ. 1983) 349, 365.
36 Gmelin Handbuch der Anorganischen Chemie, Wolfram, Erg. Bd. B2, Springer-Verlag, Berlin, 1979, p. 205.
37 A. Trumm and H. Schroecke, Neues Jahrb. Mineral. Abh., 134 (1979) 157.
38 H. Kleykamp, J. Less-Common Met., 71 (1980) 127.
39 H.J. Goldschmidt, Research, 4 (1951) 343.
40 G. Goeltz, R. Fernandez, M.A. Nicolet and D.K. Sadana, Mater. Res. Soc. Symp. Proc., 7 (1982) 227.
41 W.B. Pearson, A Handbook of Lattice Spacings and Structure of Metals and Alloys, Pergamon Press, New York, 1958.
42 Ref. 36, p. 15 ff.
43 B.D. Sawicka and J.A. Sawicki, in V. Ashworth, W.A. Grant and R.P.M. Procter (Eds.), Ion Implant Met., Proc. 3rd Int. Conf. Modif. Surf. Prop. Met. Ion Implant 1981, Pergamon Press, Oxford, 1982, p. 341 ff.
44 C.L. Herzenberg and R.D. Lamoreaux, Z. Krist., 128 (1969) 414.
45 J. Donohue, The Structures of the Elements, Wiley, New York, 1974.
46 D. Ülkü, Z. Krist., 124 (1965) 192.
47 H. Cid-Dresdner and C. Escobar, Z. Krist., 128 (1969) 414.
48 P.V. Klevtsov, N.A. Novgorodtseva and L. Yu. Kharchenko, Sov. Phys. Crystallogr., 15(3) (1970) 532.
49 J. Haber, W. Marczewski, J. Stoch and L. Ungier, Ber. Bunsenges. Phys. Chem., 79 (1975) 970.
50 F.S. Stone, J. Solid State Chem., 12 (1975) 271.
51 R. Pickering and R.J.D. Tilley, J. Solid State Chem., 16 (1976) 247.
52 R.J.D. Tilley, Chem. Scr., 14 (1978–79) 147.

53 S. Amelinckx and J. van Landuyt, in ref. 13, p. 295 ff.
54 J.R. Guenter, Proc. 10th Int. Symp. Reactivity of Solids, Dijon, France, 1984, p. 299.
55 J.R. Guenter, Mater. Sci. Monogr. (React. Solids, Pt. A), 28 (1985) 485.
56 H. Schröcke, Neues Jahrb. Mineral. Abh., 110 (1969) 15.
57 V.K. Trunov and L.M. Kovba, Izv. Akad. Nauk SSSR, Neorg. Mater., 2 (1966) 151.
58 J.R. Gavarri, D. Weigel and C. Carel, J. Solid State Chem., 29 (1979) 81; 36 (1981) 255.
59 P.P. Budnikov and A.M. Ginstling, Principles of Solid State Chemistry Reactions in Solids, Maclaren, London, 1968, pp. 108, 117, 145.
60 P.S. Mamykin, N.A. Batrakov and V.K. Bogatikova, Tr. 2nd Ural. Petrogr. Soveshch., Sverdlovsk 1966 (Publ. 1968), 7, 159–162; Chem. Abstr., 74 (1971) 104131.
61 W.M. Reiff, J.H. Zhang and C.C. Torardi, J. Solid State Chem., 62 (1986) 231.